Theoretical Studies of Potential Energy Surface and Bound States of the Strongly Bound He(1 S)−BeO (1 Σ +) Complex

ARTICLE *in* THE JOURNAL OF PHYSICAL CHEMISTRY A · JUNE 2013

Impact Factor: 2.69 · DOI: 10.1021/jp404467b · Source: PubMed

4 AUTHORS, INCLUDING:

Tatiana Korona
University of Warsaw
66 PUBLICATIONS **1,530** CITATIONS
SEE PROFILE

Grzegorz Chałasiński
University of Warsaw
152 PUBLICATIONS **4,669** CITATIONS
SEE PROFILE

THE JOURNAL OF PHYSICAL CHEMISTRY A

Article

pubs.acs.org/JPCA

Theoretical Studies of Potential Energy Surface and Bound States of the Strongly Bound He(^{1}S)−BeO ($^1\Sigma^+$) Complex

Michał Hapka,[†] Jacek Kłos,*[,‡] Tatiana Korona,[†] and Grzegorz Chałasiński[†,§]

[†]Faculty of Chemistry, University of Warsaw, Pasteura 1, 02-093 Warsaw, Poland

[‡]Department of Chemistry and Biochemistry, University of Maryland, College Park, Maryland 20742-2021, United States

[§]Department of Chemistry, Oakland University, Rochester, Michigan 48309-4477, United States

Supporting Information

ABSTRACT: We perform electronic structure calculations of the potential energy surface of the He···BeO($^1\Sigma^+$) complex. We use several different methods to characterize this unusual interaction. We apply coupled cluster singles, doubles, and noniterative triples [CCSD(T)] and the multireference configuration interaction [MRCI] levels of theory. The nature of the interaction is studied with symmetry-adapted perturbation theory (SAPT) based on DFT and CCSD description of the intramonomer electron densities. Our best estimate of the well depth is 1876.5 cm^{-1} at the CCSD(T) level, while the dissociation energy, corrected for the zero-point energy, is equal to 1446.7 cm^{-1}. The global minimum is located for the collinear He···Be−O geometry at $R_e = 4.45a_0$. The rotational constant of the He−BeO complex in its ground state is 0.863 cm^{-1}. We also calculate bound states of the He···BeO complex for $J = 0$ and $J = 1$ (total angular momentum).

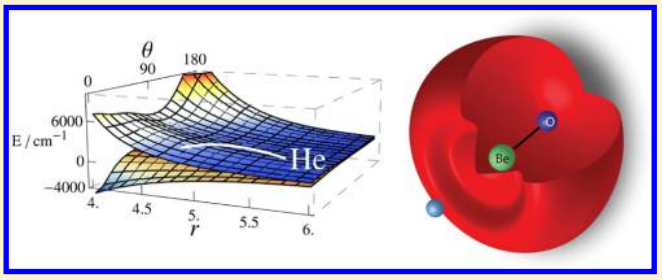

INTRODUCTION

The unusual strength of the He···BeO interaction and of similar Rg···MX complexes have fascinated researchers for almost three past decades since the pioneering ab initio work of Frenking and collaborators in the 1980s,[1,2] who placed the lower bound for the well depth astonishingly high, at a thousand wavenumbers. Later works almost doubled this result and predicted He···BeO to be an uncommon species, featuring a He···Be bond of approximately 5.3 kcal/mol.[3,4] Although IR spectra for low-temperature matrix-isolated Ar, Xe, and Kr···BeO complexes were recorded,[5] the He···BeO system has so far eluded experimental detection.[4] Moreover, the exceptional character of BeO as a Lewis acid inspired theoretical design of similar classes of helium-binding beryllium compounds.[6−8] Recent studies of unique bonding characteristic of beryllium and Group II A metals and also of Rg···BeO complexes by Heaven et al.[4] revived the interest in search for He···BeO.

The most recent accurate ab initio PES for the He···BeO complex was calculated 5 years ago by Takayanagi et al.[3] They used the CAS-PT2 method with large basis sets and included the vibrational coordinate of the BeO diatom. In our work, we provide a state-of-the-art reassessment of the potential energy surface for this challenging system by performing a variety of coupled cluster (CC) and multireference configuration interaction (MRCI) calculations. We account for the basis set superposition error (BSSE), which plays an important role in proper description of the van der Waals region in He···BeO. The first ro-vibrational levels of the complex are calculated for the CC and MRCI potential energy surfaces.

In addition, the nature of the unusual binding of He to BeO is exposed via an analysis of the symmetry-adapted perturbation theory (SAPT) interaction components. The SAPT interpretation complements previous studies on the subject, which were done by means of a topological analysis of the electron density distribution and provided an explanation in terms of donor−acceptor interactions as well as natural-bond orbitals analysis.[2,9,10]

COMPUTATIONAL DETAILS AND NUMERICAL RESULTS

The electronic ground state of the BeO molecule is described by a $^1\Sigma^+$ term. We fix the interatomic distance of the BeO molecule at $r = 1.3309$ Å, which is the experimentally determined value[11] for the ground state. The dipole moment of the BeO($^1\Sigma^+$) molecule is determined to be 2.6 a.u. (6.6 D) at the MRCISD level of theory described below. This is quite large of a dipole, suggesting that BeO is an ionically bound molecule with $Be^{2+}O^{2-}$ charge distribution.

The geometry of the He···BeO complex is described by Jacobi coordinates: distance R measured from the center of mass of the BeO molecule to the He atom, angle θ between $\vec{R}$ and diatomic vector $\vec{r}$ with $\theta = 0$ describing the collinear He···Be−O arrangement and $\theta = 180$ describing the collinear

Received: May 6, 2013
Revised: June 20, 2013
Published: June 24, 2013

He···O−Be arrangement. All calculations have been performed using the Molpro package.[12]

Below we describe results of two approaches used to obtain the two-dimensional PES for the He···BeO system. The first employs the configuration-interaction MRCISD method,[13,14] the second one uses the CCSD(T) method, i.e., the CCSD with the perturbative inclusion of triples.[15]

Multi-Reference CISD PES. To determine the two-dimensional $V(R,\theta)$ PES for the He···BeO complex, we use augmented correlation-consistent quadruple-ζ basis set (aug-cc-pVQZ) of Dunning et al.[16] for all the atoms. The reference wave functions for the multireference configuration interaction calculation with single and double excitations with a Davidson correction[17] (MRCISD+Q(Davidson)) is obtained using complete active space self-consistent field calculations (CAS-SCF) with the active space composed of 9 orbitals: 7 A′ orbitals and 2 A″ orbitals. This space includes 2s and 2p orbitals of Be. All 14 valence electrons were correlated including 1s core of Be and O.

Davidson correction lowers the size-consistency error, and the MRCISD+Q interaction energy is calculated by subtracting the total energy of the infinitely separated He and BeO monomers from the total energy of the complex at each geometry. We do not correct for the basis set superposition error (BSSE) in the MRCI calculations and assume that the BSSE is similar as in the CCSD(T) calculations described in the next subsection.

To scan the potential energy surface, we use the radial grid of 73 points spanning distances from $2.25a_0$ to $100a_0$ and the angular grid from 0 to 180° with a step of 10 degrees. The global minimum is located at $R_e = 4.43a_0$ and $\theta_e = 0°$ with a well depth of 2094.2 cm^{-1}. There is an additional local minimum for the other collinear geometry with $\theta = 180°$ corresponding to the He···O−Be arrangement, localized at $R = 6.91a_0$ and 50.7 cm^{-1} deep. There is an unusually large difference between the two collinear isomers in contrast to regular van der Waals complexes of helium. A sudden increase of the attractive region spans the angular range between $\theta = 0$ and $\theta = 40°$, a result in agreement with findings by Takayanagi et al.[3] in their CAS-PT2 studies of He···BeO. The distance between He atom and Be atom in the He···Be−O minimum is $r_{HeBe} = 2.7914a_0$. This value is similar to the position of the minimum $r = 2.7071a_0$ in the $He-Be^{2+}$ complex, which we have calculated as well (the well depth of the $He-Be^{2+}$ is equal to 7499.12 cm^{-1}).

CCSD(T) PES. We perform a similar scan of the He···BeO PES as described in the preceding subsection utilizing the CCSD(T) method. We apply aug-cc-pVQZ and aug-cc-pV5Z basis sets and correct the interaction energies for the BSSE using the standard counterpoise correction.[18] We calculate the BSSE at the Be-side to be around 270 and 23 cm^{-1} for the O-side region. We keep the 1s core orbitals correlated and doubly occupied in our CCSD(T) calculations. The T_1 diagnostic in CCSD calculations is consistently close to 0.028 for both the dimer and BeO monomer, which is slightly above the recommended value (0.02) for applications of single reference methods. This indicates a multireference character of the system.

Application of the basis set tailored for the core−valence correlation has proved to have a negligible effect, shifting the D_e value merely by 0.15%.

The global minimum for the CCSD(T)/aug-cc-pV5Z PES is equal to 1876.5 cm^{-1} and is located at $R_e = 4.45a_0$. This is 21 cm^{-1} deeper than the result obtained with the aug-cc-pVQZ basis set. Additionally, there is a local minimum for the other collinear arrangement ($\theta = 180°$), i.e., corresponding to the He···O−Be, localized at $R = 7.05a_0$ and 32.3 cm^{-1} deep. Figure 1 shows the contour plot of our CCSD(T)/aug-cc-pV5Z PES

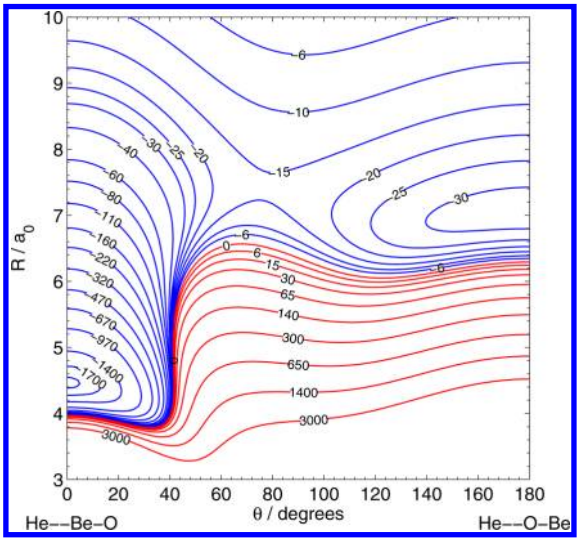

Figure 1. Contour plot of the He−BeO CCSD(T)/aug-cc-pV5Z PES. Energy contours in units of cm^{-1}.

for the He···BeO complex. We note that the MRCISD+Q PES discussed above has a very similar anisotropy; therefore, we omit showing its contour plot.

It is interesting to compare our CCSD(T) results to the CAS-PT2 predictions of Takayanagi et al.[3] In the case of the deep collinear He···Be−O minimum, we observe an excellent agreement. Their BSSE-uncorrected well depth is D_e = 1836.2 cm^{-1}, and the distance of He from Be is $2.876a_0$, which corresponds to our values of 1876.5 cm^{-1} and $R_{HeBe} = 2.841a_0$, respectively.

In their work, Takayanagi et al. do not describe the local minimum corresponding to the He···O−Be collinear arrangement. This could be attributed to the fact that CAS-PT2 is biased toward the intramonomer correlation effects and is capable of recovering only a small fraction of dispersion energy.

In Figure 5, we show the nodal isosurface of the potential energy ($V(R,\theta) = 0$) surrounding the BeO molecule. This isosurface visualizes the depletion of the repulsion energy on the Be-side of the BeO molecule; the He atom, represented by a small light-blue sphere, can approach BeO much closer than from the opposite O-side. In the following, we elucidate the nature of this peculiar anisotropy by energy partitioning via symmetry-adapted perturbation theory.

SAPT Calculations. We perform SAPT calculations based on the DFT description of the monomers.[19,20] We also test the performance of SAPT(DFT) against a recently developed SAPT(CCSD) formulation.[21−23] We apply the same basis as for MRCISD calculations. In SAPT(DFT) calculations, the PBE0 xc functional[24,25] was asymptotically corrected,[26] with vertical ionization potentials calculated using a difference method. Calculations were performed for three representative angles from the potential energy surface (0°, 90°, and 180°).

SAPT allows for a decomposition of the interaction energy in powers of the intermolecular interaction operator. By considering the perturbation expansion up to the second

dx.doi.org/10.1021/jp404467b | J. Phys. Chem. A 2013, 117, 6657−6663

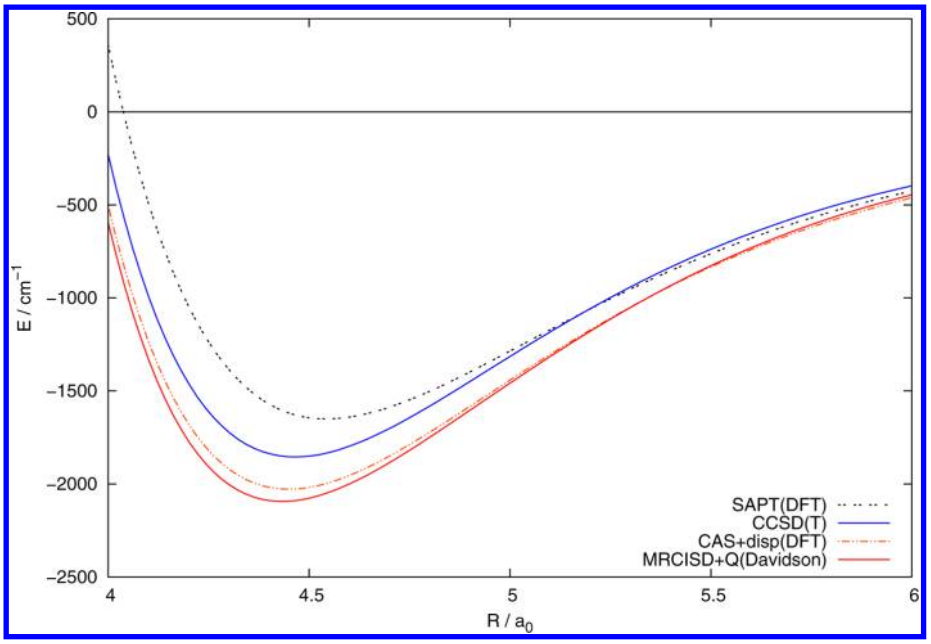

Figure 2. Interaction potentials for He···BeO, $\theta = 0°$, with different methods. See the text for description of basis sets.

order, for both SAPT(DFT) and SAPT(CCSD) methodologies, we divide the interaction energy into six physically sound energy contributions, i.e., the electrostatic and exchange energies in the first order, and induction and dispersion energies with their exchange counterparts in the second order:

$$E_{\mathrm{int}}^{\mathrm{SAPT(DFT/CCSD)}} = E_{\mathrm{elst}}^{(1)} + E_{\mathrm{exch}}^{(1)} + E_{\mathrm{ind}}^{(2)} + E_{\mathrm{exch-ind}}^{(2)} + E_{\mathrm{disp}}^{(2)} + E_{\mathrm{exch-disp}}^{(2)} \quad (1)$$

In the SAPT(DFT) method, the monomers are described by Kohn−Sham (KS) orbitals. Second-order terms are obtained from the coupled KS (CKS) theory.[19] In the SAPT(CCSD) method, the intramonomer electron correlation is accounted for at the CCSD level of theory, and therefore, SAPT(CCSD) serves as a benchmark for SAPT(DFT) calculations.[23,27]

It is often advocated[28] that SAPT up to second order should be augmented by the residual δ_{HF} term defined as

$$\delta E_{\mathrm{int}}^{\mathrm{HF}} = E_{\mathrm{int}}^{\mathrm{HF}} - (E_{\mathrm{elst}}^{(1)}(\mathrm{HF}) + E_{\mathrm{exch}}^{(1)}(\mathrm{HF}) + E_{\mathrm{ind}}^{(2)}(\mathrm{HF}) + E_{\mathrm{exch-ind}}^{(2)}(\mathrm{HF})) \quad (2)$$

where $E_{\mathrm{int}}^{\mathrm{HF}}$ stands for the Hartree−Fock supermolecular interaction energy and energy contributions are calculated at the Hartree−Fock level of theory. The purpose of the δ_{HF} correction is to account for higher-order induction effects and other residual terms.

The above SAPT(DFT) and SAPT(CCSD) approximations are known to be adequate and efficient for systems composed of monomers that are reliably described by a single-reference electronic theory. However, when monomers demand a truly multireference description (they exhibit quasi-degeneracy or the static correlation energy is large), those single-reference-based SAPT formalisms will be in trouble. Yet, beryllium and its compounds are precisely such cumbersome species. The only multireference model based on the SAPT philosophy so far is a hybrid CAS+disp method, a hybrid approach analogous to the SCF+disp hybrid method proposed by Rajchel et al.[29] (see also Kuntz et al.[30]). The CAS+disp interaction energy is defined as

$$V(R) = V^{\mathrm{CASSCF}}(R) + E_{\mathrm{disp}}^{(2)}(R) + E_{\mathrm{exch-disp}}^{(2)}(R) \quad (3)$$

Here, $V^{\mathrm{CASSCF}}(R)$ is the supermolecular interaction energy computed at the CAS-SCF level of theory, as the difference of CAS dimer and monomer energies, both obtained with a dimer-centered basis set (DCBS) to compensate for BSSE and supplemented with the residual size consistency correction (necessary for CAS calculations that do not include complete active space of the valence orbitals). Next, $V^{\mathrm{CASSCF}}(R)$ is supplemented with the dispersion energy, and the concomitant exchange-dispersion term, obtained from the SAPT calculations. The model, referred to as CAS+disp, is a direct generalization of the SCF+disp approximation of Ahlrichs et al.[31] for complexes composed of species that require more than a single configuration. It is based on an assumption that the CAS-SCF energy obtained with a limited active space is an upgrade of the SCF energy to cover primarily for static correlation effects, but only insignificantly for the dynamic portions,[30] and thus may include only a minor fraction of the dispersion component. The inability of CAS-SCF to account for the dispersion energy stems from the fact that valence space calculations optimize monomers' components of the supermolecular correlation energy rather than the interaction between them.

From the point of view of the SAPT's decomposition and nomenclature, CAS+disp accounts for the electrostatic, exchange, and induction energies, the latter summed up to infinity and accompanied by exchange effects, every term being related to the multireference rather than single reference description of monomers. The relative difference between SAPT(CCSD) and SAPT(DFT) nondispersion parts, on the one side, and the CAS-SCF interaction energy, on the other, would provide an indication and approximate quantitative measure of the multiconfiguration character of the interaction under consideration.

Comparison between SAPT(DFT) and SAPT(CCSD) results for selected geometries reveals a good agreement between both methods. In the proximity of the minimum first-order energy, contributions differ by up to few percent.

dx.doi.org/10.1021/jp404467b | J. Phys. Chem. A 2013, 117, 6657−6663

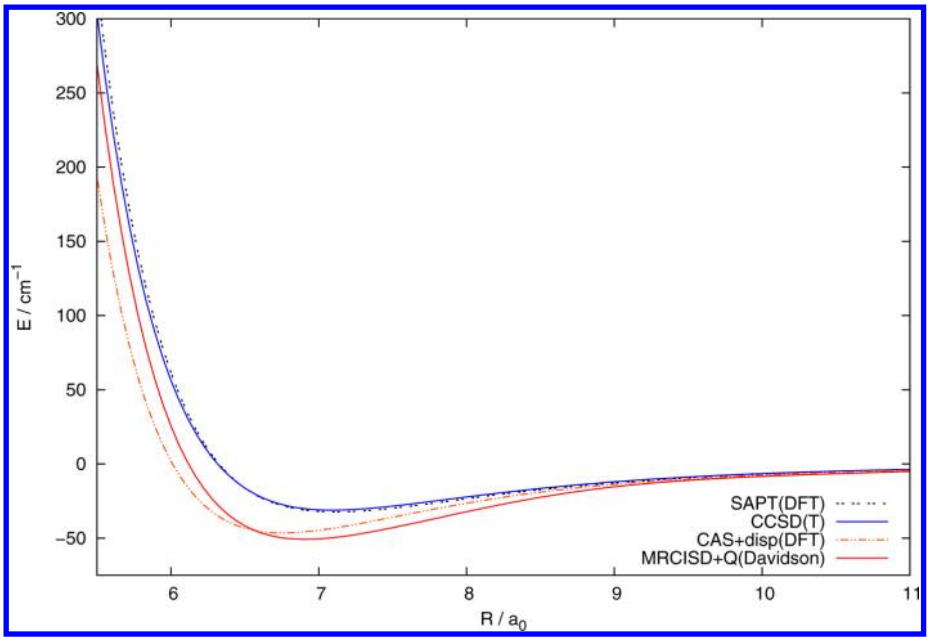

Figure 3. Interaction potentials for BeO···He, θ = 180°, with different methods. See the text for description of basis sets.

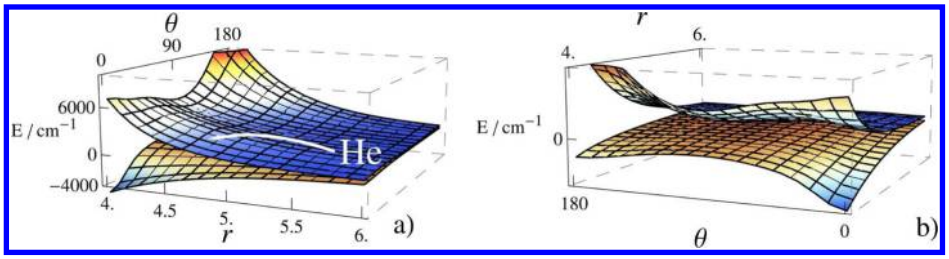

Figure 4. Exchange cavity in He···BeO visualized in two different perspectives. Upper plane shows first-order SAPT(DFT) energy. Lower plane pictures SAPT(DFT) second order energy, $E^{(2)} = E^{(2)}_{\mathrm{int,tot}} + E^{(2)}_{\mathrm{disp,tot}}$.

Furthermore, SAPT(DFT) leads to a stronger induction interaction with discrepancies reaching from 9% in the minimum up to 15% for the large distance. For a computationally demanding dispersion energy contribution, only selected distances were compared. In this case, an excellent agreement at short distance seems to deteriorate away from the minimum, with SAPT(DFT) values underestimated by 16−19% (for appropriate tables, see Supporting Information).

Moreover, we performed the additional analysis of the first-order energy contributions calculated with one-electron density matrices obtained with different methods: CAS-SCF, MRCISD, DFT(PBE0), CCSD, quadratic configuration interaction method (QCISD), and QCISD with noniterative correction to triple excitations QCISD(T).[32] The results point toward a non-negligible role of triple excitations, which in the vicinity of the global minimum reduce the repulsive character of $E^{(1)}$, therefore resembling results based on CAS-SCF densities rather than SAPT(CCSD) values (see Figure S1 in Supporting Information). In the case of the shallow local minimum for the He···OBe arrangement, the triple excitations play less significant role, which reflects in excellent agreement between QCISD(T)- and CCSD-based $E^{(1)}$ energies (Figure S2 in Supporting Information). However, one should note that the $E^{(1)}_{\mathrm{exch}}(S^2)$ formula cannot be rigorously applied to those approximate methods, which [like, e.g., MRCI or QCISD(T)] do not allow for a proper decomposition of the reduced two-particle density matrix.[22]

SAPT(DFT) with the δ_{HF} correction[19] predicts the global minimum for He···BeO at 4.542a_0 with a well depth of 1650 cm^{-1}. A large contribution of the δ_{HF} correction to the interaction energy (−266 cm^{-1} in the minimum) points toward a significant role of the induction energy in the binding of He···BeO.

The CAS+disp method predicts the minimum at 4.450a_0 with D_e = 2012.2 cm^{-1}. We show that for the crucial PES cross-section at θ = 0°, MRCISD+Q(Davidson) results remain in very good agreement with the CAS+disp model, whereas SAPT(DFT)+δ_{HF} predicts a more shallow minimum (see Figure 2).

Both methods manage to grasp the local minimum for the He···O−Be arrangement. SAPT(DFT) calculations place it at approximately 7.0a_0 and are 32.7 cm^{-1} deep. The CAS+disp approach is again closer to the MRCISD+Q prediction with R_e = 6.740a_0 and the well depth of 46.4 cm^{-1} (see Figure 3).

It is interesting to compare the performance of both SAPT(DFT) and SAPT(CCSD) methods with respect to CAS-SCF supermolecular results. In Figure 6, we see that SAPT(CCSD) supplemented with δ_{HF} fails to provide proper description of the He···BeO interaction in the vicinity of the global minimum. As pointed out earlier, one can contribute it to the negligence of higher excitations. However, SAPT-(DFT)+δ_{HF} correction agrees substantially better with CAS-SCF results. Still, the sum of first-order energy contributions, $E^{(1)}$, and second-order induction energy, $E^{(2)}_{\mathrm{ind}} + E^{(2)}_{\mathrm{exch-ind}}$,

dx.doi.org/10.1021/jp404467b | J. Phys. Chem. A 2013, 117, 6657−6663

calculated at SAPT(DFT) level recovers only 75% of the CAS-SCF energy. This, together with the magnitude of δ_{HF}, bring out the multiconfigurational character of beryllium oxide and stress the importance of taking into account higher orders of the induction energy.

SAPT analysis allows to understand the origin of the surprisingly deep minimum that occurs at a relatively short distance observed for the linear He···Be−O geometry. The large dipole moment of BeO suggests a serious deficit of a negative charge at the Be end, which manifests in dramatic reduction of the Pauli exchange repulsion, exchange cavity, on the one hand, and a severe enhancement of the induction effect on the other. A rare gas atom is pulled into this exchange cavity by the induction (dipole−induced dipole interaction) and dispersion forces, against only a gently rising repulsive Pauli barrier. For small helium, the barrier rises singularly mildly, so He may come up really close to Be, where the induction attraction becomes exceptionally large (see Figures 4 and 5).

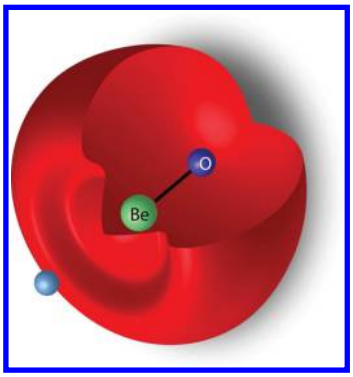

Figure 5. Exchange cavity in He···BeO visualized as a E_{int} = 0 isosurface. A quarter of the isosurface is cut out for the purpose of showing the location of the Be−O molecule.

The effect is less distinct for neon: although it senses even larger induction effect, it cannot approach so closely since the exchange cavity is smaller (i.e., exchange repulsion is far less reduced), due to the larger Ne size. As a consequence, Ne···BeO is less tightly bound and the well depth obtained with SAPT(DFT) equals 1359 cm^{-1} at R_e = 5.1a_0 (see also refs 2 and 4).

For the remaining Rg···BeO systems, i.e., Ar···BeO, Kr···BeO, and Xe···BeO, the exchange repulsion barrier steadily rises. However, because of the prevailing second-order induction and dispersion terms, SAPT predicts growing stability of the series, in accordance with CCSD(T) results (see ref 9 and Table S4 in Supporting Information).

The SAPT interaction picture can be compared to that from the atom-in-molecule (AIM) and NBO population analysis from the recent studies of Zou et al.[10] and Kobayashi et al.[9] In the work of Kobayashi et al., a decrease in the binding energy of Ne···BeO with respect to He···BeO is related to a weaker polarizability of Ne and the lack of charge balance mechanism.[9] The latter stems from the enhancement of Pauli repulsion due to $2p_\pi$ Ne and π BeO orbital interaction, a feature that is recognized in SAPT as dwindling of the exchange cavity.

Referring to the analysis of Zou et al., they attribute stabilization in the Rg···BeO series to lowering of the donor−acceptor energy gap, associated with the lone pair Rg···σ^* BeO electron delocalization.[10] Their second-order perturbation analysis[33] identifies energy contributions from individual NBOs and exposes the role of the donor−acceptor pair. Although SAPT codes do not provide any decomposition into orbital contributions, the stabilization effect in the second-order is pronounced as an increase of induction and dispersion energies.

BOUND STATE CALCULATIONS

We use the analytical Reproducing Kernel Hilbert Space fit of the MRCISD+Q(Davidson) and CCSD(T)/aug-cc-pV5Z ab initio points to calculate bound states supported by these potentials for the total angular momentum quantum number J = 0. Because of the closed shell character of the complex, we

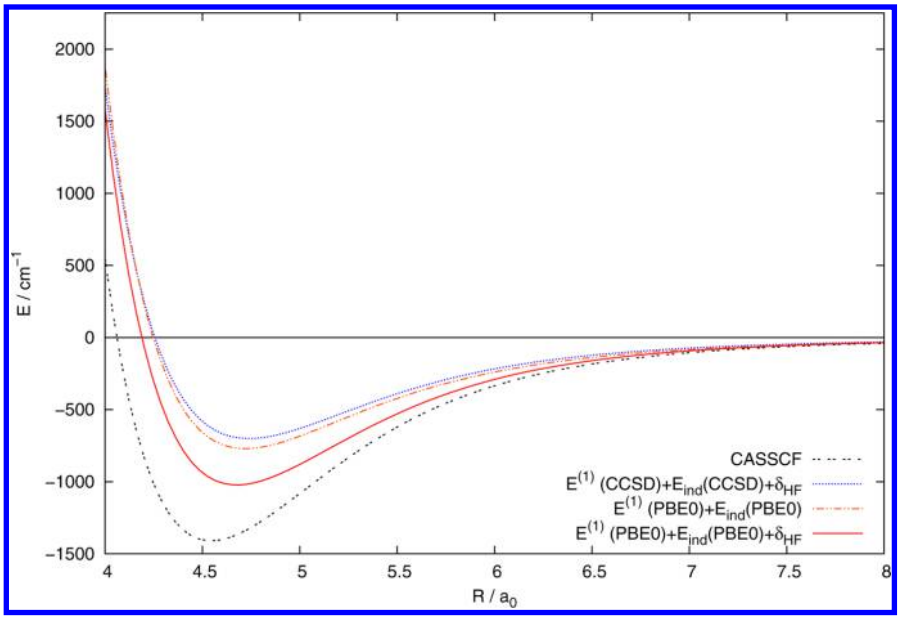

Figure 6. Comparison of CAS-SCF supermolecular energy (CASSCF) with $E^{(1)} + E_{ind}$ calculated at SAPT(DFT) and SAPT(CCSD) levels of theory. For SAPT(DFT), also, results without δ_{HF} correction are shown.

dx.doi.org/10.1021/jp404467b | J. Phys. Chem. A 2013, 117, 6657−6663

apply the collocation method to calculate bound states as described in our work on the Ar−HCN complex.[34]

In the dynamic calculations, the rotational constant of the BeO molecule is set to B_0 = 1.6415 cm^{-1}.[11] The reduced mass of the complex is 3.450345 a.m.u. corresponding to ^{4}He, ^{9}Be, and ^{16}O isotopes. To converge the bound state calculations, we use the angular grid corresponding to 30 Gauss-Legendre quadrature nodes and 150 radial nodes distributed between R = 3a_0 and 22a_0. The zero-point corrected dissociation energy in the case of the MRCISD+Q PES is 1643.5 and 1446.7 cm^{-1} for the CCSD(T)/aug-cc-pV5Z PES.

In Table 1, we list the bound states from the CCSD(T)/aug-cc-pV5Z calculations for J = 0 and J = 1 total angular quantum number. Energies of the bound states for J = 1 that appear for J = 0 are omitted. Table 1 also contains expectation values of the distance and angle associated with a given bound state and respective rotational constants of the complex. Contour plots of wave functions for selected states listed in Table 1 are presented in Figure S3 in the Supporting Information.

Table 1. Bound State Energies Based on the CCSD(T)/aug-cc-pV5Z PES and Corresponding Average Values of R and θ and Rotational Constants (Calculated from $\langle 1/R^2 \rangle$) for the J = 0 and J = 1 Total Angular Quantum Number of the He−BeO Complex[a]

(J,ν_s,ν_b)	energy	energy (ref 3)	$\langle R \rangle$ (a_0)	$\langle \theta \rangle$ (deg)	B_{rot}
(0,0,0)	−1446.66	−1377.69	4.5085	10.76	0.86329
(1,0,1)	−1264.63		4.4897	13.72	0.87071
(0,0,2)	−1089.54	−1021.63	4.4433	17.80	0.89001
(0,1,0)	−1003.74	−953.43	4.7088	11.75	0.79919
(1,0,3)	−909.92		4.4650	18.76	0.88346
(1,1,1)	−830.58		4.6639	15.13	0.81509
(0,0,4)	−738.83	−675.38	4.4228	21.58	0.90208
(0,1,2)	−669.78	−624.31	4.6614	17.79	0.82131
(0,2,0)	−634.70	−594.93	4.9301	15.37	0.73353
(1,0,5)	−557.29		4.4954	21.79	0.87962
(1,2,1)	−472.65		4.7716	20.29	0.78355
(0,0,6)	−399.33	−263.71[b]	4.4850	23.13	0.88699
(0,3,0)	−370.72	−350.45	5.0419	14.71	0.72199
(0,2,2)	−347.92	−339.96	4.9207	20.88	0.75209
(0,1,4)	−307.00	−308.13	4.8050	25.13	0.77129
(1,3,1)	−240.45		5.1333	16.51	0.69782
(0,4,0)	−168.15	−153.89	5.7417	13.37	0.56248
(0,3,2)	−119.49	−98.28	5.3449	21.42	0.64793
(0,1,6)	−84.15		4.8829	25.46	0.77282
(1,4,1)	−70.56		5.9555	20.12	0.52618
(0,5,0)	−54.01	−44.77	6.5578	19.02	0.44371
(0,3,4)	−48.03		4.8996	28.07	0.77136
(0,6,0)	−12.54		7.7997	52.39	0.31714

[a] (J,ν_s,ν_b) denote J and vibrational stretching and bending quantum numbers. For the states that appear at both values J = 0 and J = 1, we show only J = 0 values. Energies and B_{rot} in cm^{-1}. [b] Possibly a misassignment in ref 3.

It is interesting to compare our CCSD(T) bound states results with the 3-D wave packet calculations of ref 3. The values obtained by Takayanagi on the CAS-PT2 PES are 356 cm^{-1} for the (0,0,2) bending and 424 cm^{-1} for the Van der Waals (0,1,0) stretching (denoted as ν_2 and ν_3 in ref 3, respectively). On our best quality CCSD(T) PES, the (0,0,2) bending is 357 cm^{-1} and the (0,1,0) stretching equals 443 cm^{-1}, both results in excellent agreement with the study of Takayanagi.

CONCLUSIONS

The two-dimensional potential for the He···BeO($^1\Sigma$) system was determined at MRCISD+Q(Davidson)/aug-ccpVQZ and CCSD(T)/aug-cc-pV5Z levels of theory. It has been found that He···BeO exhibits a distinct multireference character; however, a single-reference CCSD(T) was able to recover accurate energy. This was not the case for single-reference SAPT calculations, which reproduced the interaction energy only semiqualitatively. A considerable quantitative improvement was obtained with the hybrid-SAPT approach: CAS+disp method, where the exchange, electrostatic, and induction parts are reproduced at the multireference level of theory.

The main features of the resulting PES were analyzed using the SAPT methodology, revealing the presence of the exchange cavity, a depletion of the exchange energy that results in a deep minimum. Such a strong interaction involving helium atom is a rare phenomenon, which has been identified only in the case of few other molecules and postulated as an example of a new type of chemical bond.[10,35]

Finally, we determined bound states and their properties supported by the CCSD(T) potential for the total angular momentum quantum numbers J = 0 and 1. We obtained a good agreement with previous CAS-PT2 potential of Takayanagi[3] with respect to the existence of a deep minimum where He approaches BeO along the Be-side. We were able to characterize a local minimum located at the O-side of BeO that was absent in the CAS-PT2 PES.

ASSOCIATED CONTENT

Supporting Information

First-order SAPT energy of He···BeO at θ = 0° and 180° calculated at different levels of theory, contour plots of selected wave functions for states listed in Table 1, second-order dispersion energies calculated at SAPT(PBE0) and SAPT-(CCSD) levels of theory, and binding energies and bond lengths of the Rg···BeO series along with basis set references. This material is available free of charge via the Internet at http://pubs.acs.org.

AUTHOR INFORMATION

Corresponding Author

*(J.K.) E-mail: jklos@umd.edu.

Notes

The authors declare no competing financial interest.

ACKNOWLEDGMENTS

J.K. would like to acknowledge the financial support through the United States National Science Foundation grant No. CHE-1213332 to M. H. Alexander. M.H. was supported by "Towards Advanced Functional Materials and Novel Devices: Joint UW and WUT International PhD Programme" Project operated within the Foundation for Polish Science MPD Programme, implemented as a part of the Innovative Economy Operational Programme (EU European Regional Development Fund). T.K. acknowledges the support from the National Science Centre of Poland through grant 2011/01/B/ST4/06141. G.C. was supported by the Polish Ministry of Science and Higher Education, Grant No. N204 248440, and by the National Science Foundation (US), Grant No. CHE-1152474.

We are thankful to Dr. Wojciech Grochala for discussion and comments.

REFERENCES

(1) Koch, W.; Collins, J. R.; Frenking, G. Are There Neutral Helium Compounds Which Are Stable in Their Ground State?: A Theoretical Investigation of HeBCH and HeBeO. *Chem. Phys. Lett.* **1986**, *132*, 330−333.

(2) Frenking, G.; Koch, W.; Gauss, J.; Cremer, D. Stabilities and Nature of the Attractive Interactions in HeBeO, NeBeO, and ArBeO and a Comparison with Analogs NgLiF, NgBN, and NgLiH (Ng = He, Ar). A Theoretical Investigation. *J. Am. Chem. Soc.* **1988**, *110*, 8007−8016.

(3) Takayanagi, T.; Motegi, H.; Taketsugu, Y.; Taketsugu, T. Accurate ab Initio Electronic Structure Calculations of the Stable Helium Complex: HeBeO. *Chem. Phys. Lett.* **2008**, *454*, 1−6.

(4) Heaven, M. C.; Bondybey, V. E.; Merritt, J. M.; Kaledin, A. L. The Unique Bonding Characteristics of Beryllium and the Group IIA Metals. *Chem. Phys. Lett.* **2011**, *506*, 1−14.

(5) Thompson, C. A.; Andrews, L. Noble Gas Complexes with BeO: Infrared Spectra of Ng−BeO (Ng = Ar, Kr, Xe). *J. Am. Chem. Soc.* **1994**, *116*, 423−424.

(6) Antoniotti, P.; Bronzolino, N.; Grandinetti, F. Stable Compounds of the Lightest Noble Gases: A Computational Investigation of RNBeNg (Ng = He, Ne, Ar). *J. Phys. Chem. A* **2003**, *107*, 2974−2980.

(7) Borocci, S.; Bronzolino, N.; Grandinetti, F. SBeNg, $SBNg^{+}$, and $SCNg^{2+}$ Complexes (Ng = He, Ne, Ar): a Computational Investigation on the Structure and Stability. *Chem. Phys. Lett.* **2004**, *384*, 25−29.

(8) Borocci, S.; Bronzolino, N.; Grandinetti, F. From OBeHe to $H_3BOBeHe$: Enhancing the Stability of a Neutral Helium Compound. *Chem. Phys. Lett.* **2005**, *406*, 179−183.

(9) Kobayashi, T.; Kohno, Y.; Takayanagi, T.; Seki, K.; Ueda, K. Rare Gas Bond Property of Rg−Be_2O_2 and Rg−Be_2O_2−Rg (Rg = He, Ne, Ar, Kr and Xe) as a Comparison with Rg−BeO. *Comput. Theor. Chem.* **2012**, *991*, 48−55.

(10) Zou, W.; Nori-Shargh, D.; Boggs, J. E. On the Covalent Character of Rare Gas Bonding Interactions: A New Kind of Weak Interaction. *J. Phys. Chem. A* **2013**, *117*, 207−212.

(11) Huber, K.-P.; Herzberg, G. *Constants of Diatomic Molecules*; Van Nostrand Reinhold: New York, 1979.

(12) Werner, H.-J.; Knowles, P. J.; Knizia, G.; Manby, F. R.; Schütz, M.; Celani, P.; Korona, T.; Lindh, R.; Mitrushenkov, A.; Rauhut, G.; et al. *MOLPRO*, version 2012.1, a package of ab initio programs; Cardiff University: Cardiff, U.K., 2012; see http://www.molpro.net.

(13) Knowles, P. J.; Werner, H.-J. An Efficient Method for the Evaluation of Coupling Coefficients in Configuration Interaction Calculations. *Chem. Phys. Lett.* **1988**, *145*, 514−522.

(14) Werner, H.-J.; Knowles, P. J. An Efficient Internally Contracted Multiconfiguration Reference CI Method. *J. Chem. Phys.* **1988**, *89*, 5803−5814.

(15) Raghavachari, K.; Trucks, G. W.; Pople, J. A.; Head-Gordon, M. A Fifth-Order Perturbation Comparison of Electron Correlation Theories. *Chem. Phys. Lett.* **1989**, *157*, 479−483.

(16) Dunning, T. H. Gaussian Basis Sets for Use in Correlated Molecular Calculations. I. The Atoms Boron Through Neon and Hydrogen. *J. Chem. Phys.* **1989**, *90*, 1007−1023.

(17) Langhoff, S. R.; Davidson, E. R. Configuration Interaction Calculations on the Nitrogen Molecule. *Int. J. Quantum Chem.* **1974**, *8*, 61−72.

(18) Boys, S. F.; Bernardi, F. The Calculation of Small Molecular Interactions by the Differences of Separate Total Energies. Some Procedures with Reduced Errors. *Mol. Phys.* **1970**, *19*, 553−566.

(19) Hesselmann, A.; Jansen, G.; Schütz, M. Density-Functional Theory-Symmetry-Adapted Intermolecular Perturbation Theory with Density Fitting: A New Efficient Method to Study Intermolecular Interaction Energies. *J. Chem. Phys.* **2005**, *122*, 014103.

(20) Misquitta, A. J.; Jeziorski, B.; Szalewicz, K. Dispersion Energy from Density-Functional Theory Description of Monomers. *Phys. Rev. Lett.* **2003**, *91*, 33201.

(21) Korona, T. Second-Order Exchange-Induction Energy of Intermolecular Interactions from Coupled Cluster Density Matrices and Their Cumulants. *Phys. Chem. Chem. Phys.* **2008**, *10*, 6509−6519.

(22) Korona, T. First-Order Exchange Energy of Intermolecular Interactions from Coupled Cluster Density Matrices and Their Cumulants. *J. Chem. Phys.* **2008**, *128*, 224104.

(23) Korona, T. Exchange-Dispersion Energy: A Formulation in Terms of Monomer Properties and Coupled Cluster Treatment of Intramonomer Correlation. *J. Chem. Theory Comput.* **2009**, *5*, 2663−2678.

(24) Perdew, J. P.; Burke, K.; Ernzerhof, M. Generalized Gradient Approximation Made Simple. *Phys. Rev. Lett.* **1996**, *77*, 3865−3868.

(25) Adamo, C.; Barone, V. Toward Reliable Density Functional Methods Without Adjustable Parameters: The PBE0 Model. *J. Chem. Phys.* **1999**, *110*, 6158−6170.

(26) Grüning, M.; Gritsenko, O.; Van Gisbergen, S.; Baerends, E. Shape Corrections to Exchange-Correlation Potentials by Gradient-Regulated Seamless Connection of Model Potentials for Inner and Outer Region. *J. Chem. Phys.* **2001**, *114*, 652−660.

(27) Korona, T. A Coupled Cluster Treatment of Intramonomer Electron Correlation within Symmetry-Adapted Perturbation Theory: Benchmark Calculations and a Comparison with a Density-Functional Theory Description. *Mol. Phys.* **2013**, *0*, 1−11.

(28) Jeziorska, M.; Jeziorski, B.; Čížek, J. Direct Calculation of the Hartree−Fock Interaction Energy via Exchange-Perturbation Expansion. The He···He Interaction. *Int. J. Quantum Chem.* **1987**, *32*, 149−164.

(29) Rajchel, Ł.; Żuchowski, P. S.; Kłos, J.; Szczęśniak, M. M.; Chałasiński, G. Interactions of Transition Metal Atoms in High-spin States: Cr, Sc−Cr, and Sc−Kr. *J. Chem. Phys.* **2007**, *127*, 244302.

(30) Kunz, C. F. Ab Initio Study of the Individual Interaction Energy Components in the Ground State of the Mercury Dimer. *Mol. Phys.* **1996**, *89*, 139−156.

(31) Ahlrichs, R.; Penco, R.; Scoles, G. Intermolecular Forces in Simple Systems. *Chem. Phys.* **1977**, *19*, 119−130.

(32) Hampel, C.; Peterson, K. A.; Werner, H.-J. A Comparison of the Efficiency and Accuracy of the Quadratic Configuration Interaction (QCISD), Coupled Cluster (CCSD), and Brueckner Coupled Cluster (BCCD) Methods. *Chem. Phys. Lett.* **1992**, *190*, 1−12.

(33) Weinhold, F.; Landis, C. R. *Valency and Bonding: a Natural Bond Orbital Donor−Acceptor Perspective*; Cambridge University Press: Cambridge, U.K., 2005.

(34) Cybulski, S. M.; Couvillion, J.; Kłos, J.; Chałasiński, G. An ab Initio Study of the Ar−HCN Complex. *J. Chem. Phys.* **1999**, *110*, 1416−1423.

(35) Grochala, W. A Metastable He−O Bond Inside a Ferroelectric Molecular Cavity: $(HeO)(LiF)_2$. *Phys. Chem. Chem. Phys.* **2012**, *14*, 14860−14868.